Cellular Signalling 25 (2013) 1962–1969

Contents lists available at SciVerse ScienceDirect

Cellular Signalling

journal homepage: www.elsevier.com/locate/cellsig

Annexin A1 is regulated by domains cross-talk through post-translational phosphorylation and SUMOYlation

Danielle Caron [a,1], Halim Maaroufi [b,1], Sébastien Michaud [a,c,d], Robert M. Tanguay [c,d], Robert L. Faure [a,*]

[a] Department of Pediatrics, Laboratory of Cellular Biology, Centre de recherche du CHUQ (Centre-Mère-Enfant Soleil), Canada
[b] Institut de Biologie Intégrative et des Système (IBIS), Canada
[c] Laboratory of Cellular and Developmental Genetics, Department of Molecular Biology, Medical Biochemistry and Pathology, IBIS, PQ, Quebec, Canada
[d] PROTEO, Université Laval, PQ, Quebec, Canada

ARTICLE INFO

Article history:
Received 20 March 2013
Received in revised form 15 May 2013
Accepted 15 May 2013
Available online 29 May 2013

Keywords:
SUMOylation
Annexin A1
Membranes
EGF receptor

ABSTRACT

Mouse prostate membrane-associated proteins of the annexin family showed changes in SUMOylation during androgen treatment. Among these the calcium-binding annexin A1 protein (ANXA1) was chosen for further characterization given its role in protein secretion and cancer. SUMOylation of ANXA1 was confirmed by overexpressing SUMO-1 in LNCaP cells. Site-directed mutagenesis indicated that K257 located in a SUMOylation consensus motif in the C-terminal calcium-binding DA3 repeat domain is SUMOylated. Mutation of the N-terminal Y21 decreased markedly the SUMOylation signal while EGF stimulation increased ANXA1 SUMOylation. A structural analysis of ANXA1 revealed that K257 is located in a hot spot where Ca^{2+} and SUMO-1 bind and where a nuclear export signal and a polyubiquitination site are also present. Also, Y21 is buried inside an α-helix structure in the Ca^{2+}-free conformation implying that Ca^{2+} binding, and the subsequent expelling of the N-terminal α-helix in a disordered conformation, is permissive for its phosphorylation. These results show for the first time that SUMOylation can be regulated by an external signal (EGF) and indicate the presence of a cross-talk between the N-terminal and C-terminal domains of ANXA1 through post-translational modifications.

1. Introduction

Annexin A1 (ANXA1) is a Ca^{2+} and phospholipid binding protein. It is involved in many important cellular processes, such as membrane trafficking, signal transduction, cellular differentiation, proliferation and cancer [1]. Most of the proteins of the annexin family are composed of two domains, the variable N-terminal domain and a conserved C-terminal core region consisting of four repeats (DA1 to DA4) of approximately 70 residues [1]. The Ca^{2+} binding sites are localized in the convex region of the C-terminal core and the flexible N-terminal domain, when positioned on the opposite concave side, allows protein–protein interactions events [1]. Studies have shown that phosphorylation, truncation or mutation of the N-terminal domain have an important impact in calcium binding in the C-terminal core and membrane binding/aggregation [2–5] suggesting the presence of a cross-talk between the N-terminal domain and the C-terminal core region.

The functions of annexins were characterized in some details in terms of membrane or actin dynamics [6–8]. They have reported functions in both the secretory [9,10] and the endocytic pathways [6]. It was shown that ANXA1 is a substrate of the EGFR tyrosine kinase [11] and is required for EGFR trafficking downstream of the substrate Hrs and the ESCRT system [12]. Several studies have also reported the role of ANXA1 in prostate cancer. Christmas et al. [13] have shown that the human prostate gland selectively secretes high concentrations of ANXA1 into the seminal plasma. The expression of ANXA1 is decreased in prostate cancer development in association with recurrence after androgen deprivation therapy [14]. It has also been shown that ANXA1 may have tumor suppression functions [15].

Protein activity is regulated by many reversible chemical modifications including covalent modifications by small ubiquitin-related modifier protein SUMO. SUMOylation can regulate protein–protein interactions, protein localization, function and turnover [16–18]. UBC9 catalyzes the formation of an isopeptide bond between the C-terminus of SUMO and the amino group of the target lysine generally within the consensus motif ψKXE/D, where ψ is a large hydrophobic amino acid and X any amino acid [19–22]. Until recently, protein

Abbreviations: SUMO, small ubiquitin-related modifier; ANXA1, annexin A1; 1-DE, one-dimensional gel electrophoresis; 2-DE, two-dimensional gel electrophoresis; DHT, 5α-dihydrotestosterone; GDX, gonadectomized; LNCaP, prostate carcinoma cell line; EGFR, EGF receptor.

* Corresponding author at: Centre de Recherche du CHUL/CRCHUQ, 2705 blvd Laurier, RC-9800, Québec, QC G1V 4G2, Canada. Tel.: +1 418 654 2152; fax: +1 418 654 2753.
E-mail address: robert.faure@crchul.ulaval.ca (R.L. Faure).
[1] Equal participation.

0898-6568
http://dx.doi.org/10.1016/j.cellsig.2013.05.028

SUMOylation has almost been solely associated with nuclear events such as transcriptional factor modification and nuclear protein transport (for reviews [20,21,23]). It was demonstrated that protein SUMOylation is also present in other compartments including the mitochondria [24,25]. Proteins involved in membrane trafficking events were also found SUMOylated [10,22,26–29].

A role for SENP1, a deSUMOylation enzyme in the development of prostate cancer was reported [30,31]. In a recent proteomic survey of the mouse prostate we identified a large pool of free SUMO-1 peptides, responsive to castration and the androgen DHT [32]. Here, a coincident profile of changes in protein SUMOylation was detectable in crude membrane and cytosol fractions. Among the SUMOylated candidates, we have identified, by two-dimensional electrophoresis (2-DE) coupled with mass spectrometry, members of the annexin family. We confirmed the SUMOylation of ANXA1 in cultured LNCaP prostate cells and have identified the major SUMOylated site in the C-terminal DA3 domains. We also found that Y21, a target of the EGF receptor (EGFR) [6], regulates the ANXA1 SUMOylation process.

2. Experimental procedures

2.1. Animals

Adult (12–15 week old, weight = 25–30 g) male C57BL6 mice, supplied by Charles River Canada Inc. (St. Constant, Canada), were maintained under standard laboratory conditions with food and water available ad libitum except that food was removed 18 h prior to organ collection. The work was conducted with the approval of Laval University Animal Care committee. Mice were assigned to 4 groups of 12 animals each. With the exception of the control group, they were gonadectomized (GDX) via the scrotal route under isoflurane-induced anesthesia 7 days prior to organ collection. Mice assigned to a control GDX group received a single subcutaneous injection of 0.2 ml 0.4% methyl cellulose/5% ethanol (vehicle) 24 h prior to organ collection while experimental groups of GDX mice received a single subcutaneous injection of DHT (5α-dihydrotestosterone at 0.1 mg/mouse, from Steraloids, Newport, Rhode Island) 24 h and 96 h prior to organ collection. The prostate (ventral and dorsal lobes) was collected and sub-cellular fractionation was processed immediately as previously described [32]. The yields of the fractions were: Crude membrane, control: 4.9 ± 0.9, GDX: 5.8 ± 1.8, DHT 24 h: 6.3 ± 1.5 and DHT 96 h: 6.5 ± 1.1 mg protein/g prostate (n = 6). Protein contents were measured using the Bradford micro-technique (#500-0006, Bio-Rad, Hercules, CA) by comparison with a BSA standard and fractions were stored at −80 °C.

2.2. Immunoblot analysis

Antibodies were obtained from various suppliers: anti-GFP (Invitrogen Life technology, Carlsbad, CA), anti-MYC (9E10) (Santa Cruz Biotechnology, Santa Cruz, CA), anti-β-galactosidase (Promega, Madison, WI), anti-EGFR, anti-p-TYR (PY20) and β-tubulin (Santa Cruz Biotechnology, Santa Cruz, CA). The anti-SUMO antibody was produced in the laboratory and its properties previously described [32]. Signals were standardized according to protein content (150 μg protein per lane) and revealed using the appropriate horseradish peroxidase-conjugated secondary antibody (Jackson ImmunoResearch Laboratories, Westgrove, PA). Membranes (PVDF) were revealed using a chemiluminescence kit (ECL, PerkinElmer life science, Boston, MA) and exposed on a Kodak film (X-Omat Blue XB-1, Kodak).

2.3. Two dimensional electrophoresis (2-DE)

Proteins from mouse membrane fraction were solubilized with 7 M Urea, 2 M Thiourea, 3% CHAPS, 80 mM DTT, 0.5% Bio-Lyte 3–10 with a trace of bromophenol blue. First dimensional protein separation was achieved by isoelectric focusing (IEF) with the Protean IEF Cell system (BioRad, Hercules, CA) using 17 cm pH 3–10 gradient IPG strip. IEF were run at 250 V constant during 15 min, 5 h of increasing voltage to get to 10,000 V and an undetermined period at 10,000 V constant to get to 30,000 V. Strips were stored at −80 °C. IPG strips were re-equilibrated using 2% DTT and 4% iodoacetamine with a trace of bromophenol blue. The second dimension separation by 11% SDS-PAGE electrophoresis was performed using the Protean Plus Dodeca cell system (BioRad, Hercules, CA). Protein visualization was made by SYPRO Ruby protein stain (BioRad, Hercules, CA).

2.4. Protein in-gel digestion

Spots matching with the immunoblot signals were extracted from gels using an automated spot cutter (ProteomeWorks spot cutter, BioRad, Hercules, CA) and placed in 96-well plates and then washed with water. Tryptic digestion and mass spectrometry analyses were performed as previously described [32].

2.5. Database searching

All MS/MS samples were analyzed using Mascot (Matrix Science, London, UK; version 2.2.0) as previously described [32]. Mascot was set up to search the *Mus musculus* Uniref100 database (version 8.0, 87,442 entries) assuming that the digestion enzyme was trypsin. Mascot was searched with a fragment ion mass tolerance of 0.50 Da and a parent ion tolerance of 2.0 Da. An iodoacetamide derivative of cysteine was specified as fixed modification. Oxidation of methionine was specified as a variable modification. Two missed cleavages were allowed. Scaffold (version Scaffold-2-05-02, Proteome Software Inc., Portland, OR) was used to validate MS/MS based peptide and protein identifications. Protein identifications were accepted if they could be established at greater than 95.0% probability and contained at least 1 identified peptide. Protein probabilities were assigned by the Protein Prophet algorithm. Proteins that contained similar peptides and that could not be differentiated by MS/MS analysis alone were grouped in order to satisfy the principles of parsimony.

2.6. Cell culture

LNCaP (LNCaP.FGC, ATCC/CRL-1740) cells were maintained in RPMI 1640 medium (HyClone) containing 10% FBS, 2.05 mM L-glutamine, 1.10^5/0.1 mg/ml penicillin/streptomycin and cultured at 37 °C in a 5% CO_2 constant atmosphere. In some experiments (Fig. 5), cells were grown in the absence of FBS 2 h before EGF stimulation (15 min, 15 ng/ml).

2.7. Cells transfection

Cells were plated 20 h in advance at a desired confluence. Cells were washed once with the culture medium and incubated 24 h in medium containing the plasmid:Fugene HD (Roche Diagnostics Canada, Laval, QC) complex (ratio 2 μg DNA: 9 μl Fugene HD) prepared according to the manufacturer's protocol. All SUMO plasmids were co-transfected with a plasmid expressing UBC9. The non-transfected (NT) control was realized using empty vector. A reporter vector pCMV-β-galactosidase (pCMVβGal CLONTECH Laboratories, Mountain View, CA) was also co-transfected to normalize transfection efficiency using a β-galactosidase assay (according to the manufacturer's protocol PROMEGA, Madison, WI). After this incubation, the medium was changed and left for another 24 h of expression before proceeding. Cellular lysates were solubilized in Laemmli sample buffer and boiled for 5 min.

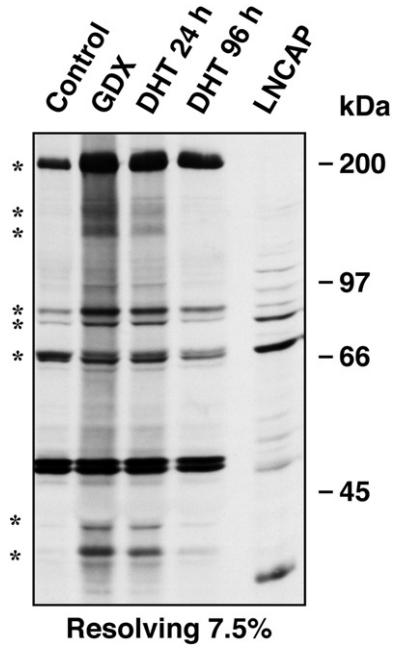

Fig. 1. Protein SUMOylation profiles in prostate fractions. Mouse membrane prostate fractions were prepared from control, castrated (GDX) and castrated mice stimulated with DHT for the indicated time (DHT). Proteins (80 μg) were separated by SDS-PAGE and transferred on PVDF membrane. Immunoblots were realized using the α-SUMO-1 antibody. Protein bands having increased signal are pointed with star symbols.

2.8. Plasmid constructs

Total cellular RNA from mouse fibroblast (MF WT) was extracted using TRIzol Reagent (Invitrogen) according to the manufacturer's instructions. Two microgram of total ARN was used to synthesize the cDNA using Omniscript reverse transcriptase (Qiagen) in a volume of 20 μl. Two microliters of this cDNA was subsequently used for PCR analysis. The pGFP-SUMO-1_{GG} and pGFP-SUMO-1Δ plasmids, expressing enhanced GFP-tagged SUMO-1 coding sequence on its constitutive active form with a diglycine group at the end (SUMO-1_{GG}) or an inactive form (G96Δ) where the glycine group has been replaced by a stop sequence (SUMO-1Δ) respectively, were realized using the complete SUMO-1 human coding sequence amplified with SUMO-1_{GG} forward primer: 5′-GATCTCGAGATGTCTGACCAGGAGGC-3′; SUMO-1_{GG} reverse primer: 5′-GCTCTAGACTAACCCCCCGTTTGTTCCTG-3′; SUMO-1Δ forward primer: 5′-GATCTCGAGATGTCTGACCAGGAGGC-3′; and SUMO-1Δ forward reverse primer: 5′-GCTCTAGACTACGTTTGTTCCTG-3′. All PCR products were digested with XhoI and XbaI, gel purified and individually inserted in pGFP-C3 vector (BD Bioscience, Mississauga, ON) at the corresponding sites previously treated with the same restriction enzymes. The plasmid pRc-CMV-UBC9 coding for UBC9 was realized using the complete UBC9 mouse coding sequence amplified with forward primer 5′-CACAAGCTTATGTCGGGGATCGCCCTC-3′ and Ubc9 reverse primer 5′-GCTCTAGATTATGAGGGGGCAAACTTCTT-3′. The PCR product was digested with HindIII and XbaI respectively, gel purified and inserted into pRc-CMV vector (Invitrogen Life technology, Carlsbad, CA) at the corresponding sites previously treated with the same restriction enzymes. The plasmid-pcDNA3-N-MYC-ANXA1 coding for ANXA1

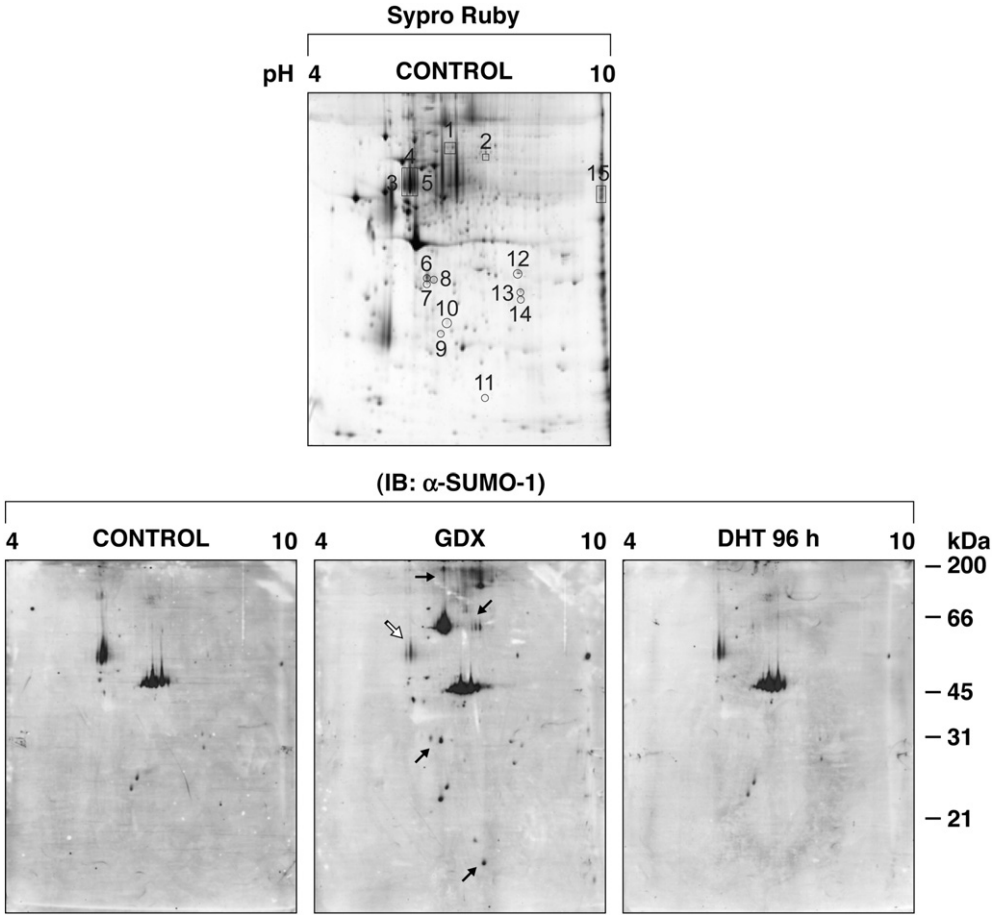

Fig. 2. 2-DE SUMOylation profiles of mouse prostate membranes. Proteins (0.5 mg; membrane fraction) were solubilized and separated by 2-DE. Protein spots were revealed by using SYPRO Ruby protein stain (upper panel). Replicated gels were submitted to the immunobloting procedure using the anti-SUMO-1 antibody (lower panels). Black and white arrows show the different protein spots that are increased (black) or decreased (white) after castration (GDX), compared to controls and after DHT treatment. Numbered spots (annexins were identified in spot 1) of interest were excised and submitted to the mass spectrometry identification procedure.

was constructed using its complete mouse coding sequence amplified using: Annexin 1 forward primer: 5′-CACGCGGCCGCTCATGGCAATGG TATCAGAATTCCTC-3′; and ANXA1 reverse primer: 5′-GCTCTAGACTAG TTTCCACCACACAGAGCCAC-3′. PCR products were digested with NotI and XbaI, gel purified and inserted into pcDNA3-N-MYC at the corresponding site to generate fusion protein bearing an N terminus MYC tag.

2.9. Site-directed mutagenesis

Mutagenesis was carried out by polymerase chain reaction (PCR). The mutations were made in the plasmid template pcDNA3-N-MYC-ANXA1 using the GeneTailor™ Site-Directed Mutagenesis System (Invitrogen Life technology, Carlsbad, CA) according to the manufacturer's protocol. Base substitution mutagenic oligonucleotide overlapping primers corresponding to position single mutants were performed for MmANXA1 on K161R, K185R, K257R and Y21F.

2.10. Immunoprecipitation (IP)

Proteins (1 mg) in Laemmli sample buffer were diluted 10 fold (50 mM Tris HCl pH 7.5, 1% NP-40, 0.25% sodium deoxycholate, 150 mM NaCl, 1 mM EDTA, 1 mM PMSF, tablet of protease inhibitor

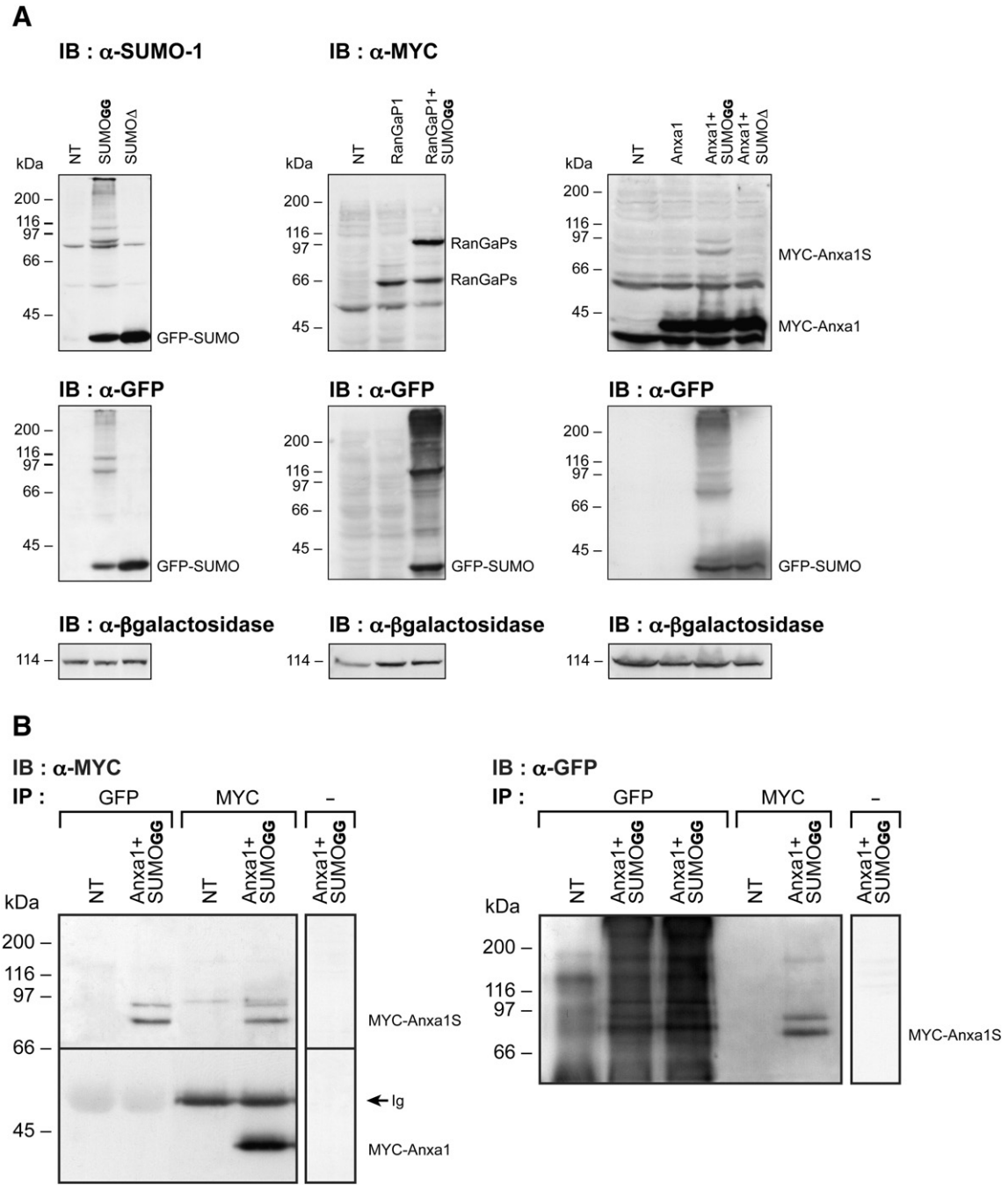

Fig. 3. SUMOylation of ANXA1 in LNCaP cells. A) LNCaP cells were co-transfected with EGFP-SUMO-1_{GG} or EGFP-SUMO-1Δ and *M. musculus* MYC-RanGAP1 or *M. musculus* MYC-ANXA1, Immunoblot (150 ug proteins) were realized using α-SUMO-1, α-GFP and α–β-galactosidase. NT = LNCaP non-transfected cells. MYC-Anxa1S: Sumoylated annexin A1. B) Immunoprecipitation (IP) of SUMOylated ANXA1. LNCaP cells co-transfected with EGFP-SUMO-1_{GG} and MYC-ANXA1. IPs (250 ug proteins) were done using α-MYC or α-GFP antibodies and protein G-Agarose beads. Proteins were separated on SDS-PAGE and immunoblotted using the α-MYC or the α-GFP antibody. The separation line indicates different exposure times of the same membrane. NT: non-transfected cells. Ig: immunoglobulins.

cocktail (ROCHE, Diagnostics, Canada, Laval, QC) prior to immunoprecipitation (IP)). IPs were performed following a pre-clearing step using protein G-Agarose (Roche Diagnostics Canada, Laval, QC), at 4 °C with constant agitation during 120 min using 2 μg of antibody of interest: anti-GFP (Invitrogen Life technology, Carlsbad, CA), anti-MYC (9E10) (Santa Cruz Biotechnology, Santa Cruz, CA). Protein G-Agarose was added for an additional 30 min. Beads were centrifuged (1 min, 12,000 *g*) and rinsed once in buffer A (50 mM HEPES pH 7.4, 1% Triton X-100, 0.1% SDS) and three times in buffer B (50 mM HEPES pH 7.4, 1% Triton X-100). Proteins were directly eluted in Laemmli sample buffer, boiled for 5 min and then stored at −20 °C prior to gel loading.

2.11. Molecular modeling

The ANXA1 model was built using the modeling software MODELLER [33]. The model was analyzed by using Ramachandran plot through PROCHECK [34]. The ANXA1 models show 98% amino acids in favored region of Ramachandran plot.

The docking of SUMO 1 in ANXA1 was performed by using the crystal 1WYW and the software Patchdock [35,36]. The latter is based on shape complementarity principles. The parameters used in this docking, clustering RMSD: 4 A complex and type: Protein–protein. The pics were generated by PyMol (http://www.pymol.org/).

3. Results

3.1. Protein SUMOylation in prostate fractions

A large pool of free SUMO-1 peptides, responsive to androgens, was previously observed in the mouse prostate [32], a tissue highly specialized in protein secretion. Immunoblot analysis with an anti-SUMO-1 antibody showed the presence in 1-DE gels of a coincident profile of protein bands, whose SUMOylation responded to hormonal treatment (Fig. 1). Immunoblot analysis of 2-DE also showed protein spots revealed with the anti-SUMO-1 antibody. Several new spots appeared or had increased intensity following castration and then returned to basal level following a single dose of DHT replacement (Fig. 2). These spots were excised for identification by mass spectrometry. 26 proteins were unambiguously identified and were classified in the intracellular trafficking, signal transduction, translation/RNA processing, cytoskeleton, metabolism, protein folding and processing categories. Hence the results indicated that the SUMOylation of a number of prostate membrane proteins was sensitive to the hormonal DHT treatment. Among the identified proteins, were members of the annexin family (spot 1, including ANXA2 and ANXA3). We chose to further analyze ANXA1 and its regulation by SUMOylation because annexins play an important role in the homeostasis of the prostate and several studies have observed the dysfunction of annexins in prostate cancer [37,38].

3.2. SUMOylation of ANXA1 in cultured cells

To validate annexin SUMOylation we used a human cell line derived from a prostate carcinoma (LNCaP) [39]. Proteins from LNCaP cells transiently transfected with GFP-SUMO-1_{GG} and SUMO-1Δ, the conjugating and conjugation deficient forms of SUMO-1 respectively were examined. Large amounts of GFP-SUMO-1 were expressed concomitantly with appearance of protein bands when the active form SUMO-1_{GG} was overexpressed (Fig. 3A, left panel). Protein SUMOylation was further validated by co-transfecting the MYC-tagged protein RanGAP1 as a positive control [40] (Fig. 3A). Co-transfections with *M. musculus* MYC-ANXA1 revealed the presence of a major 78 kDa signal. The 78 kDa signal is compatible with the presence of a complex composed of one GFP-SUMO-1 molecule (around 40 kDa) bound to the MYC-ANXA1 (around 38 kDa). A weaker 90 kDa signal was also observed in some experiments (Fig. 3A, right panel). To further confirm these results we immunoprecipitated the GFP and MYC tagged proteins before immunoblot analysis. The results confirmed robust SUMOylation of *M. musculus* MYC-ANXA1 (Fig. 3B).

3.3. Identification of the ANXA1 SUMOylation sites

We next used a site-directed mutagenesis experimental approach to identify the exact location of the SUMOylation sites on ANXA1. SUMO consensus motifs were first localized by in silico analysis. K161R, K185R, K257R mutations located in the consensus SUMO motif (ψKXE/D, respective SUMOplot™ scores: 0.91, 0.80 and 0.91) of ANXA1 were tested. The results presented in Fig. 4 confirmed the presence of the 78 kDa signal. This complex is compatible with one SUMO-1 molecule bound to the tagged ANXA1. The SUMOylation signal was not significantly affected by the K161R and K185R mutations. It was however markedly decreased by the K257R mutation (256-LKGD-259) (Fig. 4).

3.4. EGF increases ANXA1 SUMOylation

Several works have demonstrated that the N-terminal domain is particularly important for ANXA function [2–5,7,41]. Phosphorylation

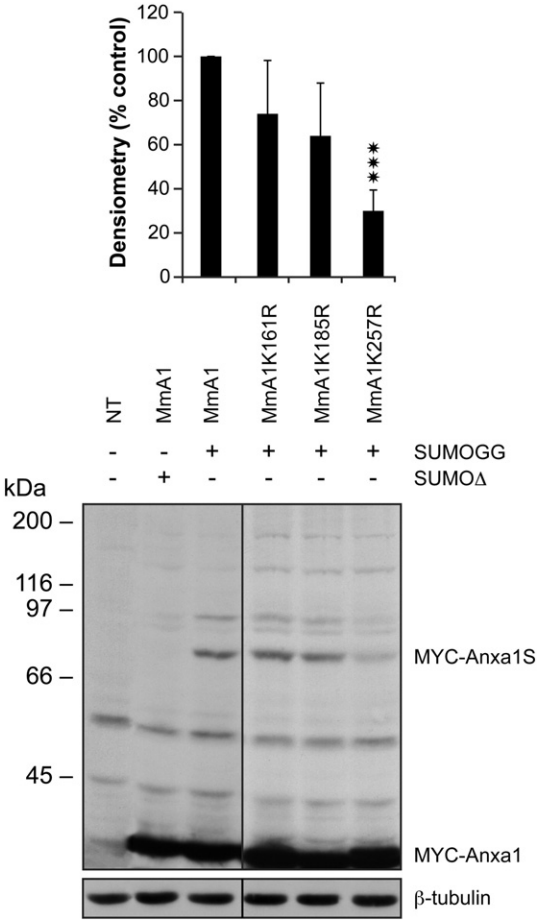

Fig. 4. Site-directed mutagenesis of ANXA1. LNCaP cells were co-transfected with the EGFP-SUMO-1Δ or EGFP-SUMO-1_{GG}.and with the wild type construct or construct bearing mutations (K257R, K161R, K185R) from predicted consensus SUMOylation sites in the *M. musculus* (Mm) MYC-ANXA1 (MmA1) DA3 domain. Proteins (150 μg) prepared in Laemmli buffer were separated by SDS-PAGE and transferred on PVDF membrane. Immunoblot were realized using an α-MYC antibody. NT = non-transfected cells. MYC-ANXA1S: SUMOylated annexin A1. Relative units were calculated from values of the mutated and wild-type (control) 78 kDa MmA1-SUMO/ANXA1 ratios and expressed as percent of control. Mean ± S.E. (n = 4), ***$p \leq 0.006$. The separation line indicates same exposure times from different pieces of gel. NT: non-transfected cells.

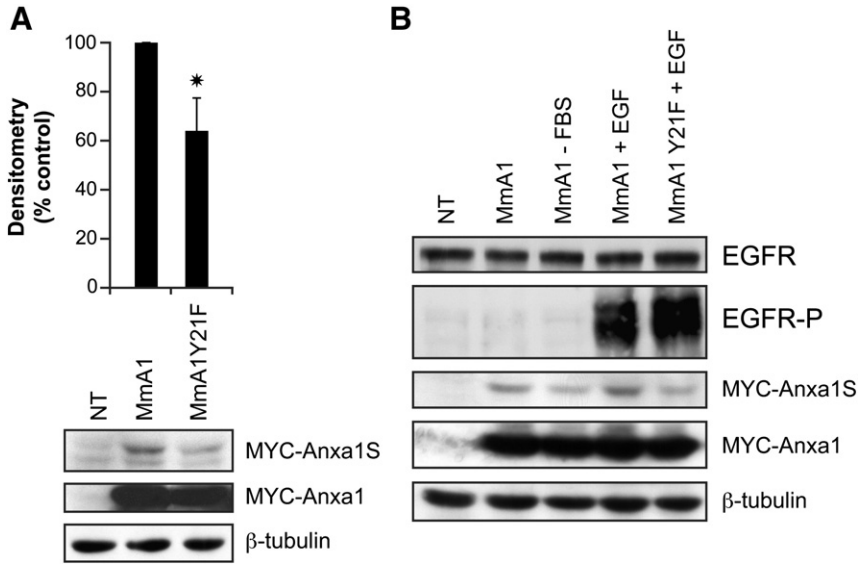

Fig. 5. Stimulation of ANXA1 SUMOylation by EGF. A) LNCaP cells were co-transfected with the EGFP-SUMO-1_{GG} and the wild type construct or a construct bearing the Y21F mutation in the N-terminal sequence of *M. musculus* (Mm) MYC-ANXA1 (MmA1). Proteins (150 ug) were separated on SDS-PAGE and immunoblotted using the α-MYC antibody. Relative units were calculated from values of the mutated and wild-type (control) 78 kDa ANXA1-SUMO/ANXA1 ratios and expressed as percent control. Mean ± S.E. ($n = 4$, $^{*}p \leq 0.02$). B) LNCaP cells were co-transfected with the EGFP-SUMO-1_{GG} and the wild type construct. Cells were cultivated in the presence or absence (two hours) of FBS and stimulated with EGF for 15 min (15 ng/ml). Proteins (150 μg) prepared in the Laemmli buffer were separated by SDS-PAGE and transferred on PVDF membrane. Immunoblots were realized using an α-MYC, α-EGFR or α-p-TYR antibody (170 kDa EGFR-P, pieces of the same membrane, representative of two independent experiments). NT = non-transfected cells. MYC-ANXA1S: SUMOylated annexin A1.

of Y- (and S-) residues in the N-terminal region regulates its function [1–3,6,12,42–45]. Indeed, it was shown that Y21 and S27 of ANXA1 are phosphorylated by protein tyrosine kinases and protein kinases A and C [6,42,46]. Given the role of annexins phosphorylation we next verified if an external signal (EGF) could regulate the SUMO-1 modification process. First we found that the Y21F mutation in ANXA1 decreased significantly by 40% the SUMOylation signal of the 78 kDa complex (Fig. 5A). We also verified if ANXA1 SUMOylation is affected after EGF stimulation. The results indicated that LNCaP cells overexpressing ANXA1 and SUMO-1 cultivated in the absence of serum for 2 h displayed an approximately 50% lower ANXA1 SUMOylation signal. In addition, following a 15 minute EGF stimulation, EGFR autophosphorylation increased markedly coincident with an increased SUMOylation signal (Fig. 5B). These data indicate that phosphorylation of tyrosine residue in the N-terminal region of ANXA1 influences the SUMOylation intensity.

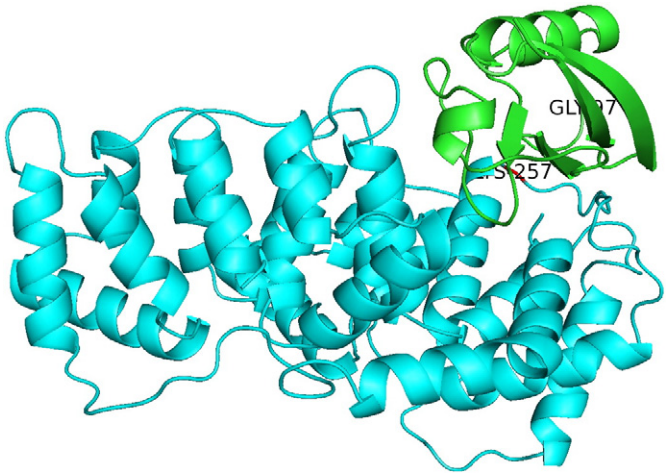

Fig. 6. Ribbon diagram of the three-dimensional structure of SUMO-1 (green) docked with *Mm* ANXA1 (blue). SUMO-1 docked with Lys257. Note that Leu256 is part of the DA3 SUMO consensus motif (LKGD). Several overlapping modulation sites implicated this region, as Ca^{2+} binding, nuclear export signal and polyubiquitination.

3.5. Molecular modeling and docking

To further understand the molecular significance of the experimental results of the K257R mutation on the SUMOylation of ANXA1, we constructed a *M. musculus* model from the *Sus scrofa* ANXA1 crystallized with and without Ca^{2+} (PDB code: 1MCX and 1HM6, respectively) [47] (Fig. 6). Human SUMO-1 (PDB code: 1WYW) was docked into the modeled MnANXA1 at K257 (Fig. 6).

The Ca^{2+} binding site located in the DE loop of DA3, is composed of D253, L256 and E261 (Fig. 6). It is interesting to note that K257 forms hydrogen bond with E261 in ANXA1 without Ca^{2+}. This bond is broken in structure with Ca^{2+}. The SUMOylation of K257 can mask calcium site of DE loop in DA3. In addition, there is a conserved leucine-rich nuclear export signal (NES) upstream to K257 ($LELK_{256}GD$; NetNes Software) where L256 is part of the SUMO consensus motif. ASAview [48] showed that Y21 situated in the N-terminal domain is buried, leading to the hypothesis that without Ca^{2+} no phosphorylation of Y21 is likely to occur [47].

4. Discussion

We found that ANXA1 was SUMOylated in prostate membrane fractions and that this modification was responsive to a hormonal treatment. Previously reported SUMO targets involved in cancer development are tumor suppressors such as p53 and the androgen receptor [49]. The expression of ANXA1 was recently associated with prostate cancer development and recurrence after androgen deprivation therapy [14]. Cheng et al. [30] have suggested a role for deSUMOylation in the development of prostate cancer. The deSUMOylating enzyme SENP1 was found over-expressed over 2-fold in human prostate cancer specimens [50]. This may explain in part the association of the counteracting deSUMOylation process and prostate cancer [30,31,51,52].

Using in silico analysis and site-directed mutagenesis, we identified K257 in ANXA1 as a major SUMOylable site. Of interest, the region where K257 is localized contains several overlapping modulation sites including a Ca^{2+} binding site, a nuclear export signal (NES), and a polyubiquitination site [53]. Hirata et al. [54] and Shimoji et al. [53] have demonstrated that SUMOylation and polyubiquitination of ANXA1 are calcium-dependent in vitro. The Ca^{2+} binding site of the DE loop of DA3 is composed of D253, L256 and E261 [47]. This later forms a hydrogen bond with K257, which is broken upon Ca^{2+} binding. Therefore the SUMOylation of K257 can mask the calcium site of the DE loop of DA3. The conformation of ANXA1 changes by Ca^{2+} binding in DA3 domain followed by the release of the N-terminal domain [47]. Varticovski et al. [42] showed that Y21 and S27 of ANXA1 are phosphorylated by protein tyrosine kinases and protein kinases A/C, respectively. Schlaepfer and Haigler [46] have reported that the equivalent of Y28, S28 is phosphorylated by protein kinase C. Solito et al. [55] demonstrated that the phosphorylated ANXA1 was translocated to the cell membrane. The Y21F mutation led here to a decreased SUMOylation of ANXA1 (Fig. 5A). On the contrary EGF increased the SUMOylation signal (Fig. 5B). It was reported that phosphorylation of Y21 in ANXA1 inhibited its ability to aggregate chromaffin granules [2,3]. Y21 phosphorylation was also shown to be involved in the docking of ANXA1 to the neck of invaginating vesicles in multi vesicular bodies (MVBs) [11,56]. ANXA1 SUMOylation may thus interfere with the inward vesiculation process of MVBs and thus late events in EGFR trafficking downstream of the substrate Hrs and the ESCRT machinery [6].

On the other hand, it was reported that SUMOylation plays an important role in the transport between the nucleus and cytoplasm. In ANXA1 there is a conserved nuclear exportation signal upstream to K257 ($LEL_{256}KGD$) where L256 is part of the SUMO consensus motif. Rhee et al. [57] reported that the presence of ANXA1 to the nucleus is favored by EGF in A549 cells. The overlapping of SUMOylation site and the putative NES region in ANXA1 suggest that SUMOylation could prevent the binding of nuclear export factors to NES so that SUMO-1–ANXA1 is retained in the nucleus [58]. In this regard, Kindsmüller et al. [59] have shown that intranuclear targeting and nuclear export of the adenovirus E1B-55K protein are regulated by SUMO-1 conjugation.

The fact that SUMOylation of K257 can also protect ANXA1 from the polyubiquitination process and thus its proteasomal degradation [60] emphasizes the idea that K257 is located in a hot spot tightly regulated through a cross-talk between the N-terminal and C-terminal domains of ANXA1.

Acknowledgments

This work was supported by grants from the Natural Sciences and Engineering Research Council of Canada (RF, OGPO157551), the Fondation des Étoiles (RF), a Studentship of the Canadian Institute of Health Research (RT) and a studentship of Health Research (DC). We thank Suzanne Fortier for expert technical assistance and Dr Michael Schwab (Laval University) for valuable comments.

References

[1] V. Gerke, S.E. Moss, Physiological Reviews 82 (2002) 331–371.
[2] E. Bitto, W. Cho, Biochemistry 38 (1999) 14094–14100.
[3] W. Wang, C.E. Creutz, Biochemistry 33 (1994) 275–282.
[4] H.T. Haigler, D.D. Schlaepfer, W.H. Burgess, Journal of Biological Chemistry 262 (1987) 6921–6930.
[5] Y. Ando, S. Imamura, Y.M. Hong, M.K. Owada, T. Kakunaga, R. Kannagi, Journal of Biological Chemistry 264 (1989) 6948–6955.
[6] C.E. Futter, I.J. White, Traffic 8 (2007) 951–958.
[7] M.J. Hayes, C.J. Merrifield, D. Shao, J. Ayala-Sanmartin, C.D. Schorey, T.P. Levine, J. Proust, J. Curran, M. Bailly, S.E. Moss, Journal of Biological Chemistry 279 (2004) 14157–14164.
[8] S. McArthur, S. Yazid, H. Christian, R. Sirha, R. Flower, J. Buckingham, E. Solito, FASEB Journal 23 (2009) 4000–4010.
[9] R. Jacob, M. Heine, J. Eikemeyer, N. Frerker, K.P. Zimmer, U. Rescher, V. Gerke, H.Y. Naim, Journal of Biological Chemistry 279 (2004) 3680–3684.
[10] W. Zhou, J.J. Ryan, H. Zhou, Journal of Biological Chemistry 279 (2004) 32262–32268.
[11] C.E. Futter, S. Felder, J. Schlessinger, A. Ullrich, C.R. Hopkins, Journal of Cell Biology 120 (1993) 77–83.
[12] I.J. White, L.M. Bailey, M.R. Aghakhani, S.E. Moss, C.E. Futter, EMBO Journal 25 (2006) 1–12.
[13] P. Christmas, J. Callaway, J. Fallon, J. Jones, H.T. Haigler, Journal of Biological Chemistry 266 (1991) 2499–2507.
[14] A.B. Smitherman, J.L. Mohler, S.J. Maygarden, D.K. Ornstein, Journal of Urology 171 (2004) 916–920.
[15] C.H. Hsiang, T. Tunoda, Y.E. Whang, D.R. Tyson, D.K. Ornstein, Prostate 66 (2006) 1413–1424.
[16] H. Lomeli, M. Vazquez, Cellular and Molecular Life Sciences 68 (2011) 4045–4064.
[17] H.D. Ulrich, A.A. Davies, Methods in Molecular Biology 497 (2009) 81–103.
[18] E.S. Johnson, Annual Review of Biochemistry 73 (2004) 355–382.
[19] C. Kretz-Remy, R.M. Tanguay, Biochemical Cell Biology 77 (1999) 299–309.
[20] S. Muller, C. Hoege, G. Pyrowolakis, S. Jentsch, Nature Reviews Molecular Cell Biology 2 (2001) 202–210.
[21] T. Sternsdorf, K. Jensen, P.S. Freemont, Current Biology 13 (2003) R258–R259.
[22] V.G. Wilson, P.R. Heaton, Expert Review of Proteomics 5 (2008) 121–135.
[23] A. Pichler, F. Melchior, Traffic 3 (2002) 381–387.
[24] E. Braschi, R. Zunino, H.M. McBride, EMBO Reports 10 (2009) 748–754.
[25] C. Figueroa-Romero, J.A. Iniguez-Lluhi, J. Stadler, C.R. Chang, D. Arnoult, P.J. Keller, Y. Hong, C. Blackstone, E.L. Feldman, FASEB Journal 23 (2009) 3917–3927.
[26] C. Denison, A.D. Rudner, S.A. Gerber, C.E. Bakalarski, D. Moazed, S.P. Gygi, Molecular & Cellular Proteomics 4 (2005) 246–254.
[27] S.R. Fuhs, P.A. Insel, Journal of Biological Chemistry 286 (2011) 14830–14841.
[28] D. Wyatt, R. Malik, A.C. Vesecky, A. Marchese, Journal of Biological Chemistry 286 (2011) 3884–3893.
[29] A. Kjenseth, T.A. Fykerud, S. Sirnes, J. Bruun, M. Kolberg, Z. Yohannes, Y. Omori, E. Rivedal, E. Leithe, Journal of Biological Chemistry 287 (2012) 15851–15861.
[30] J. Cheng, T. Bawa, P. Lee, L. Gong, E.T. Yeh, Neoplasia 8 (2006) 667–676.
[31] T. Li, S. Huang, M. Dong, Y. Gui, D. Wu, Urologic Oncology (2013), (in press).
[32] D. Caron, E. Winstall, Y. Inaguma, S. Michaud, F. Lettre, S. Bourassa, I. Kelly, G.G. Poirier, R.L. Faure, R.M. Tanguay, Journal of Proteome Research 7 (2008) 4492–4499.
[33] N. Eswar, D. Eramian, B. Webb, M.Y. Shen, A. Sali, Methods in Molecular Biology 426 (2008) 145–159.
[34] R.A. Laskowski, J.A. Rullmannn, M.W. MacArthur, R. Kaptein, J.M. Thornton, Journal of Biomolecular NMR 8 (1996) 477–486.
[35] D. Schneidman-Duhovny, Y. Inbar, R. Nussinov, H.J. Wolfson, Nucleic Acids Research 33 (2005) W363–W367.
[36] D.N.R. Duhovny, H.J. Wolfson, in: Gusfield, et al., (Eds.), Proceedings of the 2'nd Workshop on Algorithms in Bioinformatics(WABI) Rome, Italy, Lecture Notes in Computer Science, Springer Verlag, 2002.
[37] C.P. Paweletz, D.K. Ornstein, M.J. Roth, V.E. Bichsel, J.W. Gillespie, V.S. Calvert, C.D. Vocke, S.M. Hewitt, P.H. Duray, J. Herring, Q.H. Wang, N. Hu, W.M. Linehan, P.R. Taylor, L.A. Liotta, M.R. Emmert-Buck, E.F. Petricoin III, Cancer Research 60 (2000) 6293–6297.
[38] J.S. Kang, B.F. Calvo, S.J. Maygarden, L.S. Caskey, J.L. Mohler, D.K. Ornstein, Clinical Cancer Research 8 (2002) 117–123.
[39] T.M. Nicotera, D.P. Schuster, M. Bourhim, K. Chadha, G. Klaich, D.A. Corral, Prostate 69 (2009) 1270–1280.
[40] M.J. Matunis, E. Coutavas, G. Blobel, Journal of Cell Biology 135 (1996) 1457–1470.
[41] R.K. Mishra, S.S. Jatiani, A. Kumar, V.R. Simhadri, R.V. Hosur, R. Mittal, Journal of Biological Chemistry 279 (2004) 31445–31454.
[42] L. Varticovski, S.B. Chahwala, M. Whitman, L. Cantley, D. Schindler, E.P. Chow, L.K. Sinclair, R.B. Pepinsky, Biochemistry 27 (1988) 3682–3690.
[43] M. Zibouche, M. Vincent, F. Illien, J. Gallay, J. Ayala-Sanmartin, Journal of Biological Chemistry 283 (2008) 22121–22127.
[44] E.R. Eden, I.J. White, C.E. Futter, Biochemical Society Transactions 37 (2009) 173–177.
[45] M.J. Hayes, S.E. Moss, Journal of Biological Chemistry 284 (2009) 10202–10210.
[46] D.D. Schlaepfer, H.T. Haigler, Biochemistry 27 (1988) 4253–4258.
[47] A. Rosengarth, H. Luecke, Journal of Molecular Biology 326 (2003) 1317–1325.
[48] S. Ahmad, M. Gromiha, H. Fawareh, A. Sarai, BMC Bioinformatics 5 (2004) 51.
[49] R. Geiss-Friedlander, F. Melchior, Nature Reviews Molecular Cell Biology 8 (2007) 947–956.
[50] T. Bawa-Khalfe, J. Cheng, S.H. Lin, M.M. Ittmann, E.T. Yeh, Journal of Biological Chemistry 285 (2010) 25859–25866.
[51] T. Bawa-Khalfe, E.T. Yeh, Genes Cancer 1 (2010) 748–752.
[52] Q. Wang, N. Xia, T. Li, Y. Xu, Y. Zou, Y. Zuo, Q. Fan, T. Bawa-Khalfe, E.T. Yeh, J. Cheng, Oncogene 32 (2012) 2493–2498.
[53] T. Shimoji, K. Murakami, Y. Sugiyama, M. Matsuda, S. Inubushi, J. Nasu, M. Shirakura, T. Suzuki, T. Wakita, T. Kishino, H. Hotta, T. Miyamura, I. Shoji, Journal of Cellular Biochemistry 106 (2009) 1123–1135.
[54] F. Hirata, L.M. Thibodeau, A. Hirata, Biochimica et Biophysica Acta 1800 (2010) 899–905.
[55] E. Solito, H.C. Christian, M. Festa, A. Mulla, T. Tierney, R.J. Flower, J.C. Buckingham, FASEB Journal 20 (2006) 1498–1500.
[56] C.E. Futter, A. Pearse, L.J. Hewlett, C.R. Hopkins, Journal of Cell Biology 132 (1996) 1011–1023.

[57] H.J. Rhee, G.Y. Kim, J.W. Huh, S.W. Kim, D.S. Na, European Journal of Biochemistry 267 (2000) 3220–3225.
[58] W.A. Hofmann, A. Arduini, S.M. Nicol, C.J. Camacho, J.L. Lessard, F.V. Fuller-Pace, P. de Lanerolle, Journal of Cell Biology 186 (2009) 193–200.
[59] K. Kindsmuller, P. Groitl, B. Hartl, P. Blanchette, J. Hauber, T. Dobner, Proceedings of the National Academy of Sciences of the United States of America 104 (2007) 6684–6689.
[60] M.P. Kracklauer, C. Schmidt, Molecular Cancer 2 (2003) 39.